Biochemistry

 Volume 32, Number 17 May 4, 1993

Accelerated Publications

Metal Coordination Sites That Contribute to Structure and Catalysis in the Group I Intron from *Tetrahymena*†

Eric L. Christian and Michael Yarus*

Department of Molecular, Cellular, and Developmental Biology, University of Colorado, Boulder, Colorado 80309-0347

Received December 21, 1992; Revised Manuscript Received February 22, 1993

ABSTRACT: We have used nucleoside phosphorothioates (NTPαS) and a substitution-interference method to identify phosphate oxygens that appear to be important to guanosine cofactor addition in the self-splicing group I intron from *Tetrahymena thermophila*. For the majority of these phosphate oxygens, however, the effect of NTPαS substitution is significantly reduced in reactions containing the added presence of manganese ion (Mn^{2+}) relative to magnesium ion (Mg^{2+}) alone. The observed "rescue" of the NTPαS effect at these positions is thought to be due to the larger affinity of Mn^{2+} for sulfur. These data suggest the direct coordination of divalent metal ions within the highly conserved catalytic core of the *Tetrahymena* intron. Because many of these metal binding sites appear to be in positions of close backbone–backbone approach, and adjacent to the guanosine binding site the splice junction, we suggest roles for the corresponding ions in stabilizing tertiary structure and substrate recognition and as participants in catalysis.

Metal ions in RNA are not only important in determining tertiary structure but they can also provide reactive groups for RNA catalysis (Saenger, 1984; Yarus, 1993). In crystals of $tRNA^{Phe}$ at least three magnesium ions are bound to the RNA, predominately coordinating nonbridging phosphate oxygens (Holbrook et al., 1977; Jack et al., 1977; Quigley et al., 1978). These metal ions join disparate parts of the RNA sequence and stabilize sharp bends in the sugar–phosphate backbone. Other studies have shown that the binding of lead-(II) to one of the positions of Mg^{2+} coordination can catalyze the cleavage of an adjacent phosphodiester bond (Werner et al., 1976; Brown et al., 1985). Divalent metal ions are also required for the activity of a number of catalytic RNAs (Dange et al., 1990; Dahm & Uhlenbeck, 1991; Guerrier-Takada et al., 1986; Pan & Uhlenbeck, 1992; Piccirilli et al., 1993). In particular, the activity of the group I intron from *Tetrahymena* is completely dependent upon the presence of magnesium (Mg^{2+}) or manganese (Mn^{2+}) ions which are likely to play an important structural and catalytic role (Grosshans & Cech, 1989; Celander & Cech, 1991).

Substitution interference studies with phosphorothioates in the *Tetrahymena* intron have identified a number of phosphate oxygens within the intron that appear to be important to enzymatic activity. Phosphorothioates (NTPαS) are nucleotide analogs that contain sulfur in place of a nonbridging phosphate oxygen (Eckstein, 1985). When these structural probes are incorporated into RNA (strictly in the *pro-*R_p configuration), they are thought to perturb the formation of hydrogen bonds and the coordination of Mg^{2+} without a significant disruption of the secondary structure (Eckstein, 1985; Jaffe & Cohn, 1978; Pecoraro, 1984; Frey & Sammons, 1985). RNAs with multiple NTPαS substitutions (>13 NTPαS/molecule) have been used to identify five phosphate oxygens important to the attack of the CU dinucleotide at the 3′ splice site (CU addition, an analog of exon ligation) (Waring, 1989). A more sensitive approach which quantitated the effects of individual NTPαS substitution at all positions identified 44 phosphate oxygens that alter the rate of 3′ splice site hydrolysis (Christian & Yarus, 1992). In both of these studies the strongest NTPαS effects are found in regions of close backbone to backbone apposition as judged

† This work was supported by the NIH and the W. M. Keck Foundation.

0006-2960/93/0432-4475$04.00/0

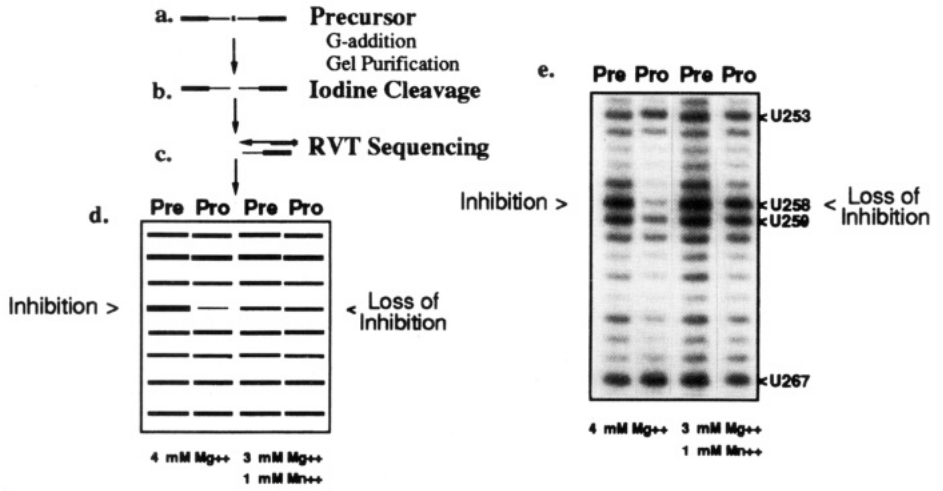

FIGURE 1: Substitution interference. Precursor RNAs containing low levels of NTPαS (see Materials and Methods) are allowed to splice in the presence of excess guanosine until 20% of the initial precursor is consumed. Splicing products are gel purified and pooled into two fractions, precursor versus all reaction products, so that reaction rate changes are only detected in the first step of splicing, G-addition. The backbone at the phosphorothioate linkage is cleaved by incubation in the presence of iodine (Schatz et al., 1991) (Figure 1b) and the position of cleavage identified by reverse transcriptase sequencing with ^{32}P end-labeled primers (Figure 1c). cDNA products are resolved on a sequencing gel where each band is representative of the level of precursor or products containing NTPαS at a specific position (Figure 1d). Comparison of single bands in precursor (Pre) and product (Pro) sequencing lanes indicates positions sensitive to NTPαS substitution. Inhibition is indicated in reactions carried out in Mg^{2+} alone by an enhancement of a specific band in the precursor lane and a corresponding reduction of the sequencing band in the same position in the product lane (Figure 1d, left lanes). The position-specific loss of inhibition in reactions carried out with the added presence of Mn^{2+} suggests a position of metal ion coordination (Figure 1d, right lanes). An example of "Mn^{2+} rescue" at positions U_{258} and U_{259} can be seen in Figure 1e. Bands observed between positions of predicted NTPαS substitution reflect experimental background due to stopping of reverse transcriptase. This background signal is subtracted when the level of the NTPαS effect is calculated (Christian & Yarus, 1992).

from the three-dimensional model of the catalytic core of the *Tetrahymena* intron proposed by Michel and Westhof (Christian & Yarus, 1992; Michel & Westhof, 1990). Our interpretation is that these NTPαS effects may indicate the position of metal ions that determine tertiary structure in the *Tetrahymena* intron. Moreover, a number of strong NPTαS effects appear to be adjacent to the guanosine binding domain and the splice junction and, therefore, could indicate ions involved in catalysis (Christian & Yarus, 1992).

In this paper, we use phosphorothioate substitution to identify structural and catalytically important Mg^{2+} binding sites throughout the phylogenetically conserved core of the group I intron from *Tetrahymena*. Specifically, we have measured the effect of NTPαS substitution on the first step of the splicing reaction, guanosine (G) addition, extending methods described previously (Christian & Yarus, 1992) and outlined in Figure 1. Positions of metal ion coordination were inferred from a comparison of modification interference studies performed with Mg^{2+} alone with those performed with the addition of Mn^{2+}. This experimental strategy takes advantage of the relative abilities of the two metal ions to coordinate oxygen and sulfur. While Mg^{2+} has been shown to have a much stronger affinity for the coordination of oxygen than sulfur [by ($>3 \times 10^4$)-fold in ATPβS], the difference in the affinity of Mn^{2+} for oxygen and sulfur is much smaller (<200-fold) (Pecoraro, 1984). Thus, substitutions found inhibitory to splicing in the presence of magnesium but not in the added presence of manganese ion (Mn^{2+} rescue) imply coordination of magnesium to a specific phosphate oxygen (Figure 1d). Since this technique is sensitive to changes in the *rate* of reaction, metal ions detected in this way directly or indirectly affect the ability to attain the transition state. We find phosphate oxygens that appear to be universally important to *Tetrahymena* RNA-based ractions as well as oxygens specifically important to G-addition. In addition, we find that the strongest NTPαS effects coincide with positions of Mn^{2+} rescue. Some of these positions of implied metal coordination appear sufficiently close to reactive bonds at the 5′ splice site to participate directly in catalysis.

MATERIALS AND METHODS

Transcription and Purification. Precursor RNAs containing the entire intron sequence from *Tetrahymena thermophila* (413 nt) and 5′ and 3′ exon sequences (42 and 82 nt, respectively) were transcribed and purified as described previously (Christian & Yarus, 1992). Briefly, 2 μg of plasmid pTT1A3 was cut with *Eco*RI and transcribed for 1–2 h in a reaction mixture (100 μL) containing 40 mM Tris-HCl, pH 8.0, 6 mM $MgCl_2$, 0.01% Triton X-100, and 5 mM dithiothreitol (DTT). In addition, reactions contained 1 mM each of ATP, CTP, GTP, and UTP and either ATPαS, CTPαS, GTPαS, or UTPαS at a level that yielded an average of two NTPαS incorporations per precursor. This level of incorporation minimizes multiple inhibitory substitutions while providing a sufficient experimental signal. Precursor RNAs were isolated on a 20-cm 5% polyacrylamide–8 M urea gel in 1 × TBE and eluted from the gel in 10 mM Tris-HCl, pH 7.5, 1 mM EDTA, 0.5 M NaCl, and 0.01% SDS overnight at 4 °C. The supernatant was precipitated twice in 2 M NH_4-OAc and 3 volumes of distilled ethanol (EtOH), resuspended in distilled H_2O, and stored at −70 °C.

Reaction Conditions. Precursor RNAs (300 nM) were renatured before splicing by heating in the presence of reaction buffer (50 mM CHES, pH 6.0, 0.2 mM EDTA,) for 3 min at 95 °C and cooled immediately on ice for at least 2 min. Metal ions (4 mM $MgCl_2$, or 3 mM $MgCl_2$ and 1 mM $MnCl_2$ final concentration) were added to reaction mixtures that were then preincubated at 37 °C for 5 min prior to reaction. Reactions were initiated by adding a molar excess of guanosine (100 μM final) and incubating until approximately 20% of the initial precursor had been consumed. Reactions were stopped by the addition of EDTA (50 mM final) and the splicing products purified as described above. Acidic conditions were used to minimize side reactions due to hydrolysis

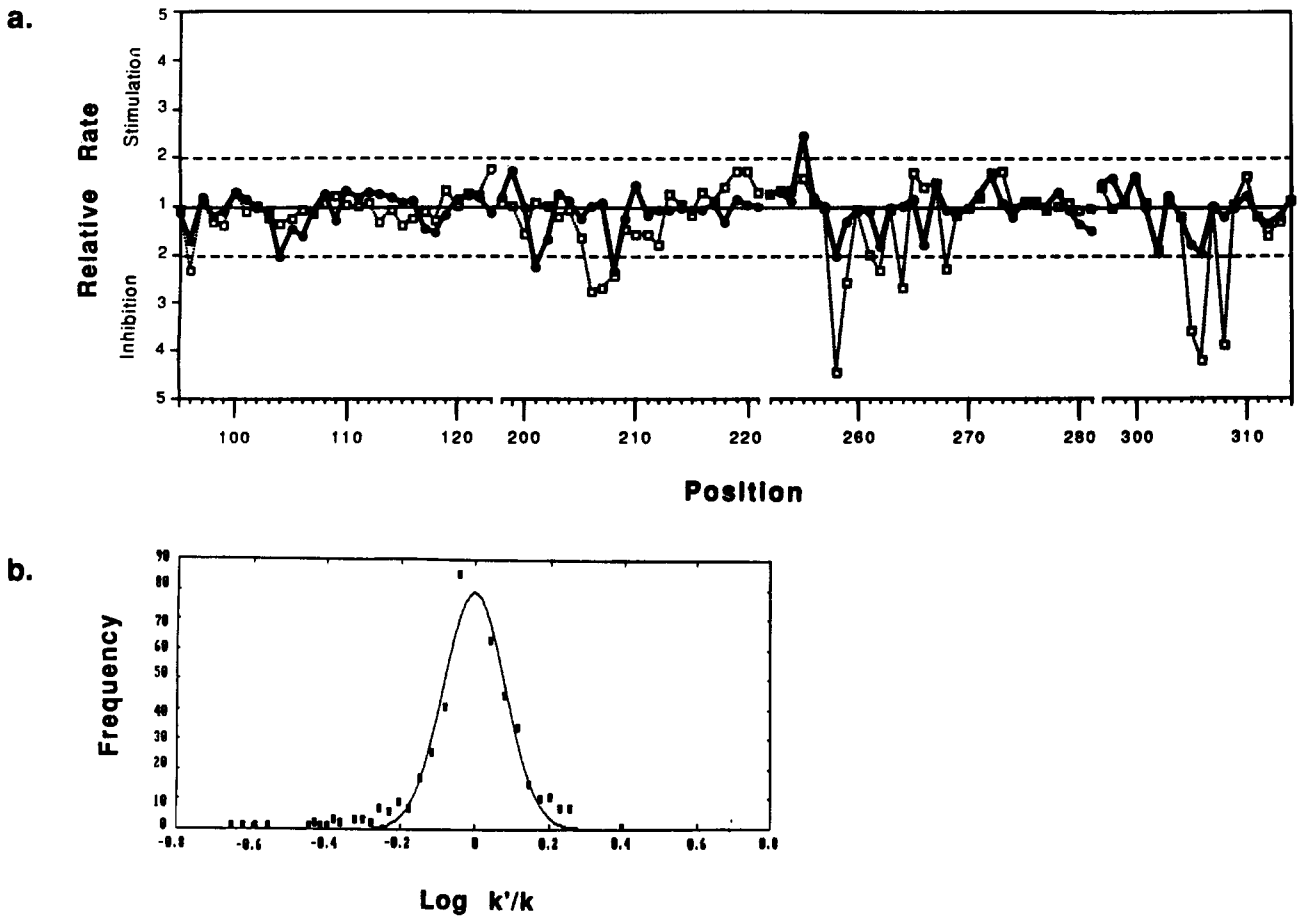

FIGURE 2: Effect of NTPαS substitution on G-addition. (a) Plot of the change in the observed rate of G-addition due to NTPαS substitution at different positions within the *Tetrahymena* intron (see below). The value 1 (dark line) indicates no change in rate, values >1 reflect x-fold stimulation, and values <1 reflect x-fold inhibition. Squares indicate reactions performed in 4 mM Mg^{2+}, and filled circles reflect reactions performed in 3 mM Mg^{2+} and 1 mM Mn^{2+}. (b) Distribution of the log of NTPαS effects. The significance of a NTPαS effect is determined from the radioactivity in sequencing bands (Figure 1d) by using an AMBIS two-dimensional radioanalytic scanner (Christian & Yarus, 1992). Since the fraction of positions strongly affected by NTPαS substitution is small (less than 10%), most band intensities in a given lane can be used to estimate the signal for an uninhibited control. The ratio of the observed band intensity at a given position to the calculated signal for an uninhibited reaction at the same position can be related directly to the change in the rate of the reaction due to NTPαS substitution at that position (Christian & Yarus, 1992). We express this change in rate as k'/k or the observed pseudo-first-order rate constant for NTPαS substitution at a single position (k') over the expected rate constant for an uninhibited reaction (k). To simplify discussion (a) plots k'/k values for NTPαS effects observed to stimulate the rate of G-addition and $(k'/k)^{-1}$ for effects observed to inhibit the rate of G-addition. NTPαS substitutions considered to have significant effects on the rate of G-addition are those whose values (Log k'/k) lie outside the normal distribution of effects (b) and in excess of the number predicted to be more than two standard deviations ($P = 0.05$) from the average effect of NTPαS substitution. Similarly, we define positions of metal ion coordination as those whose Log k'/k values (Mg^{2+} vs Mg^{2+} and Mn^{2+}) differ by more than 4 standard errors.

at the splice junctions. Partial rather than complete substitution of Mn^{2+} for Mg^{2+} was chosen to minimize structural effects due to Mn^{2+} binding at positions other than those containing NTPαS.

Analysis of Reaction Products. The identification of phosphate oxygens that alter the rate of reactions noted above was derived from a method described previously (Christian & Yarus, 1992). In short, purified precursor and pooled reaction products were cleaved at the position of NTPαS incorporation by incubation in the presence of 100 μM molecular iodine at 95 °C for 5 min, cooled on ice, and precipitated in 2 M NH_4OAc and 3 volumes of EtOH at −70 °C for at least 2 h. Cleaved splicing products were resuspended in distilled H_2O and stored at −70 °C. Sequencing reactions to determine the position of iodine-induced cleavage contained 0.5 pmol of iodine-cut precursor or splicing products and 2 pmol of 5′-^{32}P end-labeled sequencing primer in 9 μL of reverse transcriptase (RT) buffer (50 mM Tris-HCl, pH 8.3, 60 mM NaCl, 1 mM DTT). This mixture was heated for 3 min at 65 °C before addition of 1 μL of RT buffer containing 36 mM $MgCl_2$ and cooled on ice. Annealed primers were then extended with 1 unit of avian myeloblastosis virus (AMV) reverse transcriptase in the presence of 1 mM dNTPs for 5 min at 37 °C. The resulting reaction products were separated on a 40-cm 8% polyacrylamide–8 M urea sequencing gel alongside dideoxynucleotide sequencing reactions of the original pTT1A3 plasmid which served to determine the positions of iodine-induced termination of primer extension. Interpretation of sequencing banding patterns is outlined in Figures 1 and 2.

RESULTS

The effect of NTPαS substitution on G-addition in the presence of 4 mM Mg^{2+}, or 3 mM Mg^{2+} and 1 mM Mn^{2+}, is shown in Figure 2a. For reactions in the presence of Mg^{2+} alone, NTPαS substitution at most positions has little effect on G-addition, but a few positions show significant changes in rate. A plot of the log of these effects (representative of the change in free energy) vs the frequency of their occurrence (Figure 2b) demonstrates that a number of positions lie outside the normal distribution of NTPαS effects. We identify 28 positions as significant, that is, in excess of the number that

should be more than 2 standard deviations from the center of the normal distribution of effects (Figure 2b). However, half of these significant effects change the rate of G-addition by less than 2-fold. In fact, even more subtle kinetic and structural information may be contained within the data shown in Figure 2a where we reproducibly observe regions of slight enhancement or inhibition. In this initial analysis, however, we restrict discussion to the most significant NTPαS effects: those having a 2-fold effect or greater on the observed rate constant for reactions with G (dashed lines Figure 2a). These positions are G_{96}, A_{206}, A_{207}, C_{208} U_{258}, U_{259}, A_{261} C_{262}, G_{264}, A_{268}, U_{305}, A_{306}, and A_{308}.

At positions of metal ion coordination, we expect the added presence of Mn^{2+} ion to generally reduce the level of the NTPαS effect observed in the presence Mg^{2+} alone. Indeed, this is observed for the majority of these larger NTPαS effects (9/13) at positions A_{206}, A_{207}, U_{258}, U_{259}, G_{264}, A_{268}, U_{305}, A_{306}, and A_{308} (Figure 2). Position A_{261} is also likely to be a position of metal rescue. Although this position shows complete rescue on gels, the level of inhibition in the presence of Mg^{2+} is small and thus can only be considered significant with a 90% probability that this value is distinct from the normal distribution of NTPαS effects. At one position outside the catalytic core, G_{201}, the presence of Mn^{2+} ion causes inhibition that is not observed in the presence of Mg^{2+} alone. The presence of "Mn^{2+} inhibition" is not unexpected since Mn^{2+} may coordinate a different subset of atoms in RNA than Mg^{2+} (Holbrook et al., 1977). Thus, the Mn^{2+} inhibition may be due to altered RNA structure near this one site.

Within the catalytic core, however, NTPαS and Mn^{2+} rescue effects appear to be attributable to the inhibition of Mg^{2+} binding at the site of sulfur substitution. If Mg^{2+} binding is inhibited, then higher levels of Mg^{2+} ion should compensate for the ion's reduced affinity for sulfur. Higher levels of Mg^{2+} in these reactions do, in fact, rescue smaller NTPαS effects (data not shown). Mn^{2+}, like Mg^{2+}, can assume an octahedral coordination geometry (Gray, 1973), is active in G-addition and other reactions of the *Tetrahymena* intron, and is likely to occupy Mg^{2+} binding sites and to employ phosphate oxygens in its coordination sphere (Grosshans & Cech, 1989). Although the exact coordination of Mn^{2+} can be somewhat different from Mg^{2+} (Jack et al., 1977), our results are consistent with the reestablishment of direct (inner sphere) metal ion coordination by Mn^{2+} at sites of sulfur substitution.

DISCUSSION

The positions of significant NTPαS effects on G-addition as well as the inferred positions of direct metal coordination are shown on the two-dimensional model of the *Tetrahymena* intron in Figure 3. Positions of NTPαS effects and Mn^{2+} rescue occur within the highly conserved sequences in the group I core. Very strong NTPαS and Mn^{2+} effects can be seen adjacent to bases A_{308} (in helix P7) and A_{306} (in the adjacent single-stranded region, J8/7), nucleotides that are more than 90% conserved among known group I introns (Michel & Westhof, 1990). Positions of NTPαS effects and Mn^{2+} rescue are also seen adjacent to the universally conserved G_{264}, which constitutes a portion of the guanosine binding site (Michel et al., 1989; Yarus et al., 1991a,b). In addition, these sites are seen adjacent to the universally conserved bases A_{261}, in the single-stranded region connecting helices 6 and 7 (J6/7), and A_{207} in loop L4, whose functions in splicing remain unknown (Michel & Westhof, 1990). The clustering of NTPαS effects and the positions of metal ion coordination are particularly evident when these effects are viewed on the

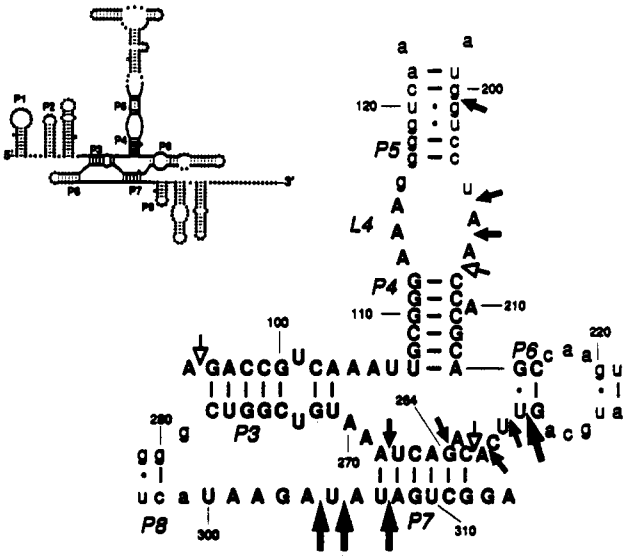

FIGURE 3: Positions of NTPαS effects and implied positions of metal ion coordination on the two-dimensional model of the *Tetrahymena* intron. The small drawing represents the complete *Tetrahymena* intron. The darkened region indicates the location of the expanded region shown to the right. Upper-case letters reflect nucleotides of the phylogenetically conserved core. All arrows indicate positions of NTPαS effects that change the observed rate of G-addition by 2-fold more. Larger arrows indicate rate changes of 3-fold or more. Filled arrows indicate positions of implied metal ion coordination.

three-dimensional model of the *Tetrahymena* core developed by Michel and Westhof (1990) (Figure 4). Both NTPαS effects and positions of implied metal coordination are particularly concentrated near the guanosine binding domain and the splice junction.

A number of these NTPαS positions have been detected in all reactions studied by the substitution interference method. In particular, clear NTPαS effects are seen at positions U_{305}, A_{306}, and A_{308} for G-addition, CU-addition to the 3′ splice site (Waring, 1989), and 3′ splice site hydrolysis (Christian & Yarus, 1992). In addition, NTPαS substitution at U_{258}, U_{259}, and G_{264} shows very strong effects on G-addition and 3′ splice site hydrolysis. In CU addition reactions NTPαS at U_{258} and U_{259} produced little effect; however, these effects could have been obscured by high levels of NTPαS substitution (Waring, 1989; Christian & Yarus, 1992). G_{264} was not studied in the CU addition experiments. Positions which appear consistently important to activity are intriguing candidates for essential tertiary structure and/or catalytic function.

Certain NTPαS effects are specific for G-addition. Most notably, NTPαS substitution at A_{206}, A_{207}, and C_{208} inhibits G-addition strongly but does not detectably inhibit CU-addition at the 3′ splice site and only weakly inhibits ($k/k' \ll$ 2-fold) 3′ splice site hydrolysis. This is consistent with the finding from photo-cross-linking studies that suggests that position A_{207} of loop L4 is positioned close to both the bound guanosine cofactor (Wang & Cech, 1992) and the splice junction (Wang et al., 1993). These positions on the ribozyme are likely to be involved specifically in the binding or activation of the guanosine or the exon (see below).

The finding that the strongest NTPαS effects correlate not only with positions of Mn^{2+} rescue but also with the regions of close backbone apposition predicted in the Michel–Westhof three-dimensional model (1990) of the *Tetrahymena* intron suggests a role for the corresponding ions in stabilizing tertiary structure. In this model, the backbones at positions U_{305} and A_{308} approach each other by virtue of a sharp bend in the

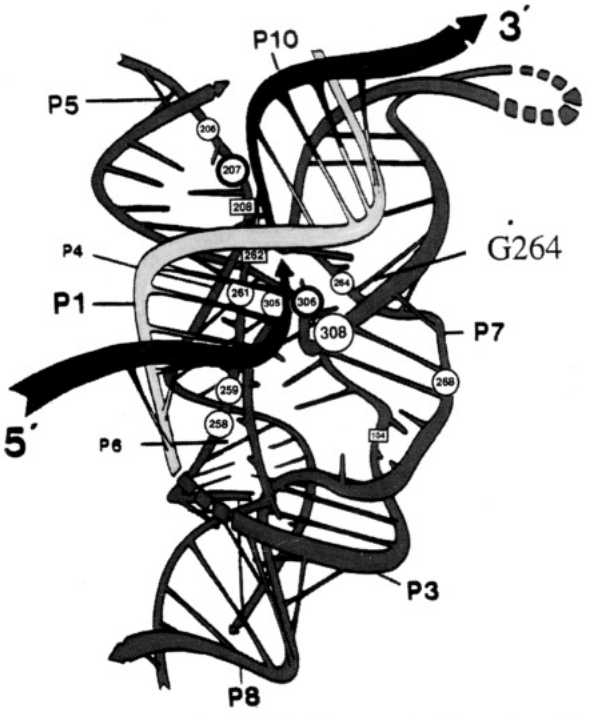

FIGURE 4: Positions of NTPαS effects on the three-dimensional model of the *Tetrahymena* core. The *Tetrahymena* core is represented as two helical domains: coaxially stacked helices P7, P3, and P8 (right) and a portion of helix 5, helix P4, and helix P6 (left back). Between these domains, 5′ and 3′ exon sequences are contained within helices P1 and P10, respectively, and are shown coaxially stacked in order to bring the 5′ and 3′ splice junctions together close to the guanosine binding domain (Michel et al., 1989; Yarus et al., 1991a,b) (adjacent to nucleotides 263–265). Squares denote NTPαS effects of 2-fold or greater on the rate of G-addition. Circles denote NTPαS effects that are also positions of implied metal ion coordination. Circles with darker outlines (positions 207 and 306) reflect candidates for metal ions involved in catalysis. Figure adapted from Michel and Westhof (1990) with permission.

chain between these two positions. Our results are consistent with the possibility of a single metal ion that stabilizes this sharp bend in the RNA backbone in a manner analogous to that observed in the sharp turn formed between the aminoacyl and D-stem in yeast $tRNA^{Phe}$ (Quigley et al., 1978). The model also predicts that the backbone at G_{264} closely approaches the backbone at the base of helix P4 and the single-stranded region J3/4 where we observe smaller effects on hydrolysis. The metal ion we observe to be coordinated to position G_{264} of the guanosine binding domain may stabilize an interaction between these backbone oxygens and join the guanosine binding domain to the rest of the ribozyme. Similarly, phosphate oxygens at positions U_{258} and U_{259} in helix P6 and the adjacent single-stranded region J6/7 are thought to closely approach the backbone of J8/7 near base A_{302} where we also observe a smaller but significant effect (k'/k = 1.9) on G-addition. Such an interaction could be stabilized by metal ions that appear to be coordinated to positions U_{258} and U_{259}.

A number of positions of apparent metal ion coordination also appear to be on the interface between the catalytic core and the RNA substrate. Strong NTPαS effects at U_{305}, A_{306}, and A_{308} fall in positions thought to be adjacent to the backbone of the last two nucleotides of the 5′ exon in helix P1, while the positions of NTPαS effects associated with A_{206} and A_{207} are close to the first nucleotides in the 3′ exon of helix P10. Each of these positions appears to be involved in metal ion coordination. Thus, the simplest interpretation is that, as in $tRNA^{Phe}$, Mg^{2+} ion allows the assembly of negatively charged domains into complex three-dimensional structures. Moreover, these results suggest that, in addition to base pairing and hydrogen bonding to sugar hydroxyls, ribozymes such as that from *Tetrahymena* may use metal ion coordination or a "metal bridge" in the recognition of nucleic acid substrates.

Changes in *catalytic* metal ion coordination can affect all RNA-catalyzed reactions because in the metal-depleted RNA the metal-catalyzed step becomes rate-limiting. Indeed, the positions at which we observe the strongest NTPαS effects (U_{259}, U_{305}, A_{306}, and A_{308}) are also those that appear to be universally important to activity in the *Tetrahymena* intron. The level of product formation approaches background when NTPαS is substituted at these positions. Therefore, we quote only a lower limit for the effect at these positions (Christian & Yarus, 1992). The actual level of NTPαS effects at the most sensitive positions may be much larger.

Biochemical evidence suggests that three of the positions that appear to be universally important to activity, U_{305}, A_{306}, and A_{308}, are close to the splice junction since they are tethered at their 5′ end by a tertiary interaction between the base at A_{302} and the 2′-hydroxyl of U_{-3} (Pyle et al., 1992) and at the 3′ end by the guanosine binding domain contained in helix P7. Of these three positions, the Michel–Westhof three-dimensional model (1990) places phosphate oxygens at position A_{306} closest to the 5′ splice site. The metal ion associated with A_{306} appears close enough to directly coordinate the 3′ oxygen of the cleavage site and thus may act to stabilize the exon leaving group in G-addition. Interestingly, the substitution of the bridging oxygen of the leaving group with sulfur has a large effect on the rate of cleavage of the L-21 ribozyme (Piccirilli et al., 1993). Moreover, this effect is rescued with the addition of Mn^{2+} ion. These experiments imply that metal ion coordination may act to stabilize the developing negative charge at the 3′ ribose oxygen (or sulfur) as part of the transition state of the reaction. Thus, the *pro-*R_p oxygen of A_{306}, as part of a highly conserved group I geometry, may anchor this catalytically important metal ion to the active center of the ribozyme.

In a different experimental approach, the backbone adjacent to A_{306} has been shown to be cleaved by Mn^{2+}, Ca^{2+} (T. S. McConnell, unpublished data), and Pb^{2+} (Streicher et al., 1993) in solutions of *Tetrahymena* precursors and L-21 ribozyme, respectively. Although this does not identify the site of metal ion coordination or imply participation in any step in the splicing reaction, a specific cleavage does support a metal binding site near the splice junction. Interestingly, Fe^{2+} (Wang & Cech, 1992) has been observed to induce cleavage of the backbone adjacent to position A_{207} where we observe both Mn^{2+} rescue and NTPαS effects that appear specific to the G-addition reaction. Moreover, mutations at A_{207} strongly affect (ca. 18-fold) the chemical step of the G-dependent endonuclease reaction of the L-21 ribozyme (A. M. Pyle and F. L. Murphy, unpublished results). In addition to a metal ion that stabilizes the leaving group (3′O) in G-addition, it has been suggested (Piccirilli et al., 1993) that a second metal ion may activate the ribose of the guanosine nucleophile. These observations in conjunction with the cross-linking studies that place the A_{207} region of loop L4 close to the bound guanosine cofactor (Wang & Cech, 1992) and splice junction (Wang et al., 1993) suggest a catalytic role for the metal ion we detect at position A_{207}. In the current three-dimensional model, however, a metal ion coordinated to position A_{207} is somewhat distant from the cleavage site and thus may interact indirectly through the coordination of water, or the conformation of the *Tetrahymena* ribozyme during

G-addition may be somewhat different than during the exon ligation step modeled by current three-dimensional structure.

Metal ions have also been implicated in the cleavage mechanisms of two other natural RNA catalysts. In RNase P, the M1 RNA–tRNA enzyme–substrate complex can form in the absence of divalent cation but is catalytically inactive (Smith et al., 1992). In the hammerhead ribozyme, NTPαS substitution at the cleavage site strongly inhibits the cleavage reaction in the presence of Mg^{2+} ion but not in the presence of Mn^{2+} ion, implying direct coordination of Mg^{2+} ion to the *pro-*R_p oxygen at the cleavage site as a requirement for catalysis (Dahm & Uhlenbeck, 1991). These results indicate that the *Tetrahymena* ribozyme, like other known RNA catalysts, functions as a metalloenzyme and support the notion that metal ions are a central feature of RNA active sites (Yarus, 1993).

ACKNOWLEDGMENT

We thank Dr. Francois Michel and Dr. Eric Westhof for the coordinates of their three-dimensional model of the *Tetrahymena* group I core. We also thank Dr. Gregg Connell, Dr. Jonatha Gott, and Dr. Dennis Schultz for invaluable discussion and comments and Dr. Robin Gutell for his help in generating Figure 3.

REFERENCES

Brown, R. S., Dewan, J. C., & Klug, A. (1985) *Biochemistry 24*, 4785–4801.

Celander, D. W., & Cech, T. R. (1991) *Science 25*, 401–407.

Christian, E. L., & Yarus, M. (1992) *J. Mol. Biol. 228*, 743–758.

Dahm, S. C., & Uhlenbeck, O. C. (1991) *Biochemistry 30*, 9464–9469.

Dange, V., van Atta, R. B., & Hecht, S. M. (1990) *Science 248*, 585–588.

Eckstein, F. (1985) *Annu. Rev. Biochem. 54*, 367–402.

Frey, P. A., & Sammons, P. (1985) *Science 228*, 541–545.

Gray, H. B. (1973) *Chemical Bonds*, pp 152–164, Benjamin/Cummings Publishing Co., London.

Grosshans, C. A., & Cech, T. R. (1989) *Biochemistry 28*, 6888–6894.

Guerrier-Takada, C., Haydock, K., Allen, L., & Altman, S. (1986) *Biochemistry 25*, 1509–1515.

Holbrook, S. R., Sussman, J. L., Warrant, R. W., Church, G. M., & Kim, S. H. (1977) *Nucleic Acids Res. 4*, 2811–2820.

Jack, A., Ladner, J. E., Rhodes, D., Brown, R. S., & Klug, A. (1977) *J. Mol. Biol. 111*, 315–328.

Jaffe, E. K., & Cohn, M. (1978) *J. Biol. Chem. 253*, 4823–4825.

Meyer, S. L. (1975) in *Data Analysis for Scientists and Engineers*, p 224, John Wiley & Sons Inc., New York.

Michel, F., & Westhof, E. (1990) *J. Mol. Biol. 216*, 585–610.

Michel, F., Hanna, M., Green, R., Bartel, D. P., & Szostak, J. W. (1989) *Nature 342*, 391–395.

Pan, T., & Uhlenbeck, O. C. (1992) *Biochemistry 31*, 3887–3895.

Pecoraro, V. L. (1984) *Biochemistry 23*, 5262–5271.

Piccirilli, J. A., Vyle, J. S., Caruthers, M. H., & Cech, T. R. (1993) *Nature 361*, 85–88.

Pyle, A. M., Murphy, F. L., & Cech, T. R. (1992) *Nature 358*, 123–128.

Quigley, G. J.,. Teeter, M. M., & Rich, A. (1978) *Proc. Natl. Acad. Sci. U.S.A. 75*, 64–68.

Saenger, W. (1984) in *Principles of Nucleic Acid Structure*, pp 201–219, Springer-Verlag Inc., New York.

Schatz, D., Leberman, R., & Ecktein, F. (1991) *Proc. Natl. Acad. Sci. U.S.A. 88*, 6132–6136.

Smith, D., Burgin, A. B., Haas, E. H., & Pace, N. R. (1992) *J. Biol. Chem. 267*, 2429–2436.

Streicher, B., von Ashen, U., & Schroeder, R. (1993) *Nucleic Acids Res. 21*, 311–317.

Wang, J. F., & Cech, T. R. (1992) *Science 256*, 526–529.

Wang, J. F., Downs, W. D., & Cech, T. R. (1992) *Science* (in press).

Waring, R. B. (1989) *Nucleic Acids Res. 17*, 10281–10293.

Werner, C., Krebs, B., Kieth, G., & Dirheimer, G. (1976) *Biochim. Biophys. Acta 432*, 161–175.

Yarus, M. (1993) *FASEB J. 7*, 31–39.

Yarus, M., Illangesekare, M., & Christian, E. L. (1991a) *Nucleic Acids Res. 19*, 1297–1304.

Yarus, M., Illangesekare, M., & Christian, E. L. (1991b) *J. Mol. Biol. 222*, 995–1012.